Progress in Earth and Planetary Science

RESEARCH ARTICLE Open Access

Soil salinity assessment by using near-infrared channel and Vegetation Soil Salinity Index derived from Landsat 8 OLI data: a case study in the Tra Vinh Province, Mekong Delta, Vietnam

Kim-Anh Nguyen[1,2,3], Yuei-An Liou[1*], Ha-Phuong Tran[4], Phi-Phung Hoang[3,5] and Thanh-Hung Nguyen[6]

Abstract

Salinity intrusion is a pressing issue in the coastal areas worldwide. It affects the natural environment and causes massive economic loss due to its impacts on the agricultural productivity and food safety. Here, we assessed the salinity intrusion in the Tra Vinh Province, in the Mekong Delta of Vietnam. Landsat 8 OLI image was utilized to derive indices for soil salinity estimate including the single bands, Vegetation Soil Salinity Index (VSSI), Soil Adjusted Vegetation Index (SAVI), Normalized Difference Vegetation Index (NDVI), and Normalized Difference Salinity Index (NDSI). Statistical analysis between the electrical conductivity ($EC_{1:5}$, dS/m) and the environmental indices derived from Landsat 8 OLI image was performed. Results indicated that spectral values of near-infrared (NIR) band and VSSI were better correlated with $EC_{1:5}$ (r^2 = 0.8 and r^2 = 0.7, respectively) than the other indices. Comparative results show that soil salinity derived from Landsat 8 was consistent with in situ data with coefficient of determination, R^2 = 0.89 and RMSE = 0.96 dS/m for NIR band and R^2 = 0.77 and RMSE = 1.27 dS/m for VSSI index. Findings of this study demonstrate that Landsat 8 OLI images reveal a high potential for spatiotemporally monitoring the magnitude of soil salinity at the top soil layer. Outcomes of this study are useful for agricultural activities, planners, and farmers by mapping the soil salinity contamination for better selection of accomodating crop types to reduce economical loss in the context of climate change. Our proposed method that estimates soil salinity using satellite-derived variables can be potentially useful as a fast-approach to detect the soil salinity in the other regions with low cost and considerable accuracy.

Keywords: Soil salinization, Near-infrared (NIR), Climate change, Electrical conductivity, Landsat 8 OLI, Tra Vinh Province, Mekong Delta

Introduction

Salinity intrusion affects agricultural activities in many parts of the world (Suarez 1989; Shammi et al. 2019). It has become a pressing issue in the Mekong Delta of Vietnam, which has been ranked among top five countries most likely to be affected by climate change coupled with sea level rise. Depending on the emissions pathway, it is estimated that about 6–12 million people will be potentially affected by coastal flooding by 2070–2100 and climate change will reduce the national income by up to 3.5% by 2050 (World Bank Group 2018). In particular, Tra Vinh Province characterized by low-lying coastal and river delta region is of very high vulnerability to saline intrusion, fluvial flooding, and cash crops. This area is experiencing effects of annual monsoon of tropical climate zone with long rainy season that source of salt brought from the sea by the tides and sea level rise. This region's climate is also impacted by the EI

* Correspondence: yueian@csrsr.ncu.edu.tw
[1]Center for Space and Remote Sensing Research, National Central University, No. 300, Jhongda Rd., Jhongli District, Taoyuan City 32001, Taiwan, Republic of China
Full list of author information is available at the end of the article

Niño Southern Oscillation (ENSO), which influences monsoonal circulation, showing enhanced influence of sea level rise and drought (World Bank Group 2018). That is to say, soil salinization is a dynamic phenomena, which can occur through a natural process (primary salinization due to sea level rise) or as a result of human activities (secondary salinization due to urbanization or irrigation) of enriching the soil with soluble salts to deteterious levels at or near the soil surface (Metternicht et al. 2008; Gorji et al. 2017), resulting in modification of biochemical features of soil. Salinity intrusion occurs when salts are dissolved in water and accumulated in the soil at a level that affects agricultural production, environment, and economics. During the initial phase, salinity affects the metabolism of soil organisms and reduces the productivity of land. In the next phase, it destroys all the plants and other organisms living in the soil. Salinity intrusion is thus one of the influencial factors leading to land degradation and triggering a significant threat on the sustainable growth and economic benefits (Wiegand et al. 1994; Sertel and Tanik 2017). Globally speaking, it is estimated that farmland affected by salinity is approximately 45 million hectares with an increased rate from 200,000 to 500,000 hectares a year (CGIAR 2016). In Vietnam, according to recent report of Directorate of Water Resources (DWR)-Ministry of Agriculture and Rural Development (MARD), the discharge of water in the upstream of the Mekong River was reduced to 900 m^3/s. Meanwhile, the water level in the middle and downstream of Mekong River was increased by 0.1–1.5 m. The intrusion of seawater increases salinity of water surface by about 4 g/l spreading through Hau and Tien Rivers, deep into to 45–65 km and 55–60 km from the coast, respectively (Nguyen and Tanaka 2007; Nguyen et al. 2008; Nowacki et al. 2015). In contrast, the drought led to a decline in underground water level and salinity intrusion in the sweeping 90 years, focusing primarily in Tra Vinh, Ben Tre, and Kien Giang Provinces. In addition, according to the report of DWR-MARD in Tra Vinh Province, in the dry season in 2016, 12,346 ha of rice were damaged due to the impact of drought and salinity intrusion, mainly in the Tra Cu, Cau Ngang, Tieu Can, Chau Thanh, and Duyen Hai districts and Tra Vinh City (CGIAR 2016) Provincial Report of Tra Vinh, 2011-2015.

Because of the devastating impacts of salinization on soil fertility and agricultural production, finding ways to mitigate the negative impacts on the soil is essential. A prime step is to map its spatial extent and classify the severity of salinity in the affected areas for sustainable agricultural planning. Ultilizing the satellite data and remote sensing techniques for monitoring soil salinity has become more efficient and economical (Dehni & Lounis 2012; Taghadosi et al., 2018, Seghal et al, 1988. Different approaches have been developed and utilized such as spectral reflectivity, combined spectrum channels, statistical analysis, mathematical modeling, and geophysical measurements. Fernandez-Buces et al. (2006) Among the various satellite sensors and techniques used to map salinity and produce EC maps, multispectral satellite imagery has been widely studied in the literature and found to be a very promising tool for mitigating this type of task (Richards 1954; Sehgal et al. 1988; Prentice 1972; Richardson et al. 1976; Dwivedi and Rao 1992; Dwivedi and Sreenivas 1998). Verma et al. (1994) studied soil contamination and found that the degree of soil contaminated by salt affects the land cover characteristics, resulting in different appearances (color, texture, shape, etc.) on the Landsat TM images. Ivits et al. (2013) addressed the limitation of productivity of salt-affected soils across the European continent by using soil maps and SPOT time series satellite images. Scudiero et al. (2015) used Landsat ETM+ canopy reflectance for assessing soil salinity at region scale. In most cases, multiple bands were transformed into a single index that is more sensitive to soil salinity than a single band (Madani 2005; Fernandez et al. 2006; Weng et al. 2010; Aldakheel 2011; Allbed et al. 2014; Zhang et al. 2015; Fan et al. 2015). Results of these studies indicated the high possibility of mapping salinity using Landsat data. Recently, Landsat TM/ETM+ data have been used to monitor a variety of environmental issues for overall vulnerability assessment (Nguyen et al. 2016; Liou et al. 2017). This served as a base to develop a global map of eco-environmental vulnerability (Nguyen and Liou 2019a) with methodology detailed in Nguyen and Liou (2019b) and a conceptual framework to further examine vulnerability and adaptive capacity (VAC) using geospatial techniques at regional scales, applied over Vietnam (Nguyen et al. 2019.) Furthermore, Sommerfeldt et al. (1984) and Douaoui et al. (2006) investigated the correlation between indices derived from Landsat 8 OLI images and amount of salt obtained from in situ data. Sommerfeldt et al. (1984) used different techniques to analyze the salinity of the soil. Their research confirmed that salty soil can be reasonably well detected by using Landsat data. Douaoui et al. (2006) compared 11 indices derived from satellite imagery with 20 m resolution collected during the 1997 summer sampling campaign and found that regression–kriging systematically provided the best validation statistics (bias, accuracy, rank of method), while vegetation indices (NDVI) was proven to be poor predictors of soil salinity within this context. In contrast, Sumfleth and Duttmann, 2008 modified a method for predicting the arrangement of land bases in paddy rice fields by utilizing in situ data and satellite

information as an index number. Their correlation analysis showed that the distribution of salt content has a close relationship with NDVI and that it substantially corresponded to the terrain features such as relative altitude, e.g., the altitude of drainage channel, and topographical wetness. Several studies explored the potential of soil salinity mapping by using very high spatial resolution (VHSR), i.e., QuickBird and IKONOS imageries through vegetation indices (Setia et al. 2013; Allbed et al. 2014; Sidike et al. 2014). However, the major limitation of VHRS is not freely available and, thus, not economic to apply for large areas. Additionally, Tao et al. (2012) retrieved soil salt content (SSC) from the Advanced Land Imager (ALI) multi-spectral image based on generalized regression neural network (GRNN). Partial least squares regression (PLSR) model has been widely used in estimation of soil parameters (Farifteh et al. 2007; Zhang et al. 2011; Nawar et al. 2014). Goldshleger et al. (2012) integrated passive and active remote sensing methods for assessing soil salinity. Yang et al. (2015) used a dataset of 92 points with salt data at depth of 30–40 cm that was divided into two subsets for prediction and validation.

In general, the techniques and methods used in the previous studies to extract soil salinity information from satellite images have been successful to some extent. However, the study of soil salinity in the low-lying coastal plain where tidal effects associated with topographical conditions and sea level rise, for instance, Mekong Delta, is relatively poorly investigated. Hence, we used simultaneous sampling soil data with Landsat 8 image acquisition. Soil samples were analyzed to obtain $EC_{1:5}$, and the coefficient of determination between $EC_{1:5}$ of soil content and spectral reflectance bands at the location of the sampling points on Landsat 8 were investigated. Based on the two sources of data, regression analysis was performed to relate satellite remote sensing data and ground measured salinity to derive the soil salinity map for Tra Vinh Province. This method can rapidly assess the soil salinity for the whole Mekong Delta less commonly found in the previous studies,

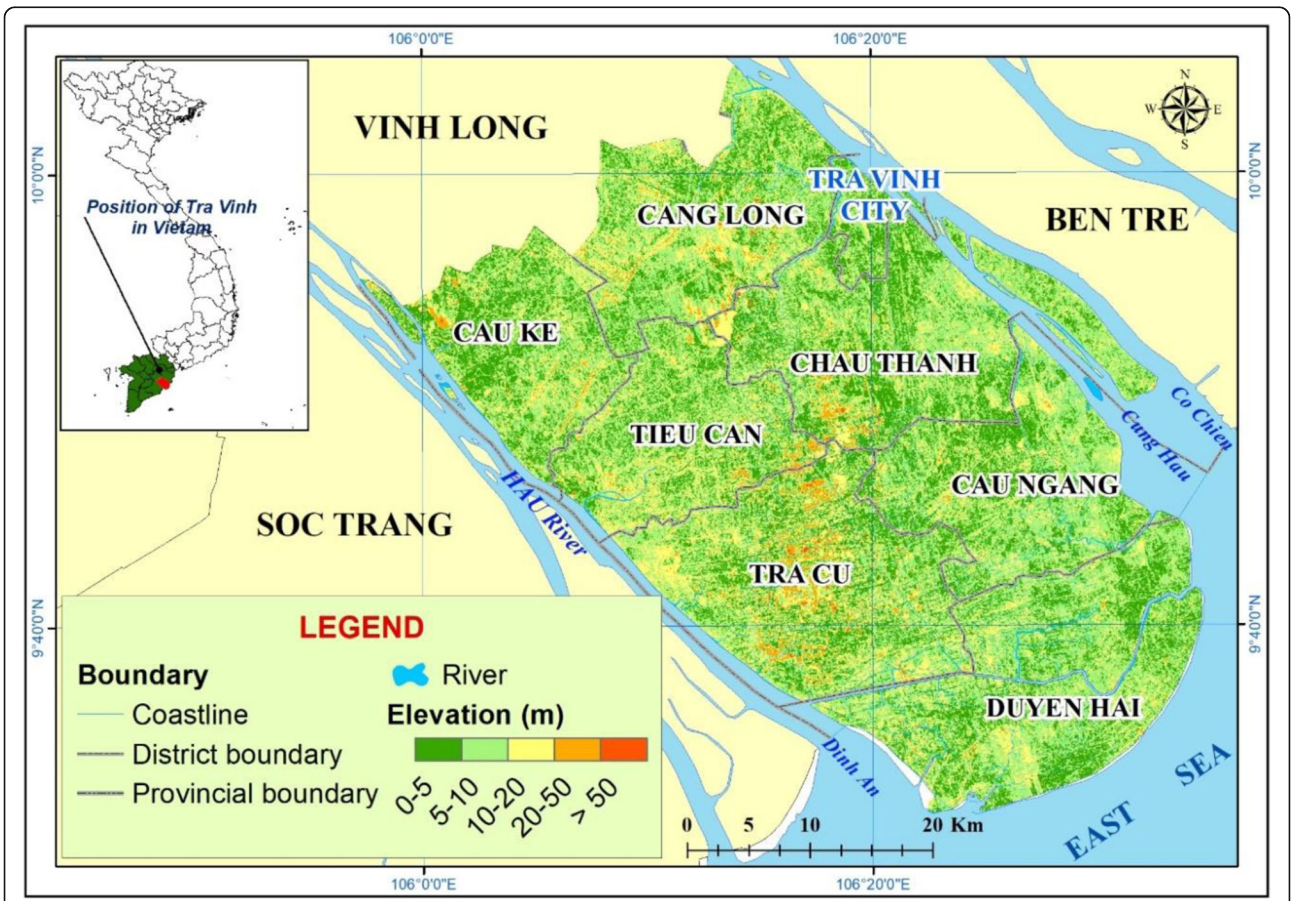

Fig. 1 Geographical location of Tra Vinh Province in the Mekong Delta, Vietnam, and DEM of Tra Vinh Province was built from terrain data with scale of 1/5000 (Source: Vietnam Department of Surveying and Mapping, 2008)

Table 1 Classification of soil salinity based on electrical conductivity values (http://vro.agriculture.vic.gov.au/dpi/vro/vrosite.nsf/pages/water_spotting_soil_salting_class_ranges#)

$EC_{1:5}$ (dS/m)	Soil salinity classes
< 2	No salinity
2–4	Low salinity
4–8	Medium salinity
8–16	High salinity
> 16	Very high salinity

especially under continuous drought and seawater conditions rising in this coastal plain.

Methods/Experimental

Study area

The Tra Vinh Province is selected for this study (Fig. 1). Its geographical location ranges from 9° 31′ 46″ N to 10° 04′ 05″ N and from 105° 57′ 16″ E to 106° 36′ 04″ E, covering an area of 2341.2 km^2. Tra Vinh is characterized by the lower delta terrain, belonging to the last point of downstream of the Mekong River with an average elevation ranging from 0.6 m to 1.0 m (occupying 66% of the area of the province). Its soil is attributed by high sediments mainly deposited due to annual flooding. Its sedimentations were from the river and sea to form alluvial plains, lowland, swamp, and sand dunes. The sand dunes have an average height of 1.0 m to 3.0 m, particularly with heights of up to 5.0 m in Long Son and 10 m in Long Toan. For example, high altitude terrains in the Tra Vinh Province can be seen in Fig. 1. Located in the tropical monsoon climate, Tra Vinh's climate is divided into two distinct seasons, namely rainy and dry seasons. The rainy season starts from May to October with prevailing wind of southwest monsoon and causes heavy rain. The dry season starts from November to April. In a year, rainfall is unevenly distributed, forming two distinct seasons corresponding to the monsoon regime in the area. The rainy season associated with the southwest monsoon starts in May and ends in October. At Cang Long weather station, the average rainfall in the rainy season is 1617 mm with less annual fluctuation. The dry season is associated with less damping northeast winds, starting in November and ending in April of the next year. The average dry season rainfall is 198 mm and fluctuates significantly through the season. The temperatures in the area are relatively high (26–27.6 °C), while their difference is not much during the season. The lowest temperature in a year falls in January and the highest temperature is in April. The average humidity in a year is 83–85 %. The driest months are in February and March. Average evapotranspiration varies from 48 mm in July to 111 mm in March. The highest evapotranspiration occurs in the dry season from December to April, during which timeframe rainfall is negligible. The Tra Vinh Province is directly affected by the semi-tide regime of the East Sea through the Co Chien River and Hau River (Provincial Report in 2011–2015). The tidal effect gradually decreases from the sea to the inland, mainly in coastal areas. The tide also causes negative consequences of salinity intrusion into the interior, changing the quality of soil in the direction of increased salinity.

Saline water intrudes into Tra Vinh simultaneously with the tide regime, depending on the seasons of the year, generally highest in March, April, and May. According to observation data, the salinity is about 25–32 g/l at the gates of Cung Hau and Dinh An. On the pedology side (Fig. 2), land of Tra Vinh Province is dominated by alluvial soils and acid sulphate soils, with 56% of saline-affected soils and 24.3% of acid soils, including three major soil groups: (i) sandy soil has an area of 15,169.3 hectares, mainly distributed in Tra Cu, Cau Ngang, Duyen Hai, and Chau Thanh districts and scattered in the other districts ; (ii) alluvial land covers an area of 132,983.4 hectares, primarily distributed along sand dunes and concentrated in Cau Ngang, Tra Cu, Duyen Hai, and Chau Thanh; and (iii) acidic soil area is 55,719.4 hectares, mainly distributed in Cang Long and Cau Ke with some scattered in Tieu Can, Chau Thanh, and Tra Vinh town.

Groundwater in coastal areas of Tra Vinh Province exists in two forms, namely shallow groundwater and deep groundwater. The shallow groundwater is under the sand dunes. The water source is mainly from local rainwater stored as groundwater with depth of less than 100 m and small reserves. The deep groundwater also known as Pleistocene groundwater is at depth of more than 100 m. The water source is enough, around 97,000 m^3/day, for daily life and living with ability to exploit.

Materials

(1) Landsat 8 OLI satellite image Level 1T product with radiometrically corrected and co-registered to a cartographic projection and terrain corrections acquired on February 14, 2017, with a resolution of 30 m.

(2) Field salinity survey was conducted by taking soil samples over Tra Vinh Province. In total, 44 soil samples, between 0 and 20 cm depths, were collected with 41 of them used in this study since 3 samples were eliminated due to their locations being underneath of cloudy sky. The locations of samples were selected based on the soil classification map of Tra Vinh Province (Fig. 2) to meet the requirement that

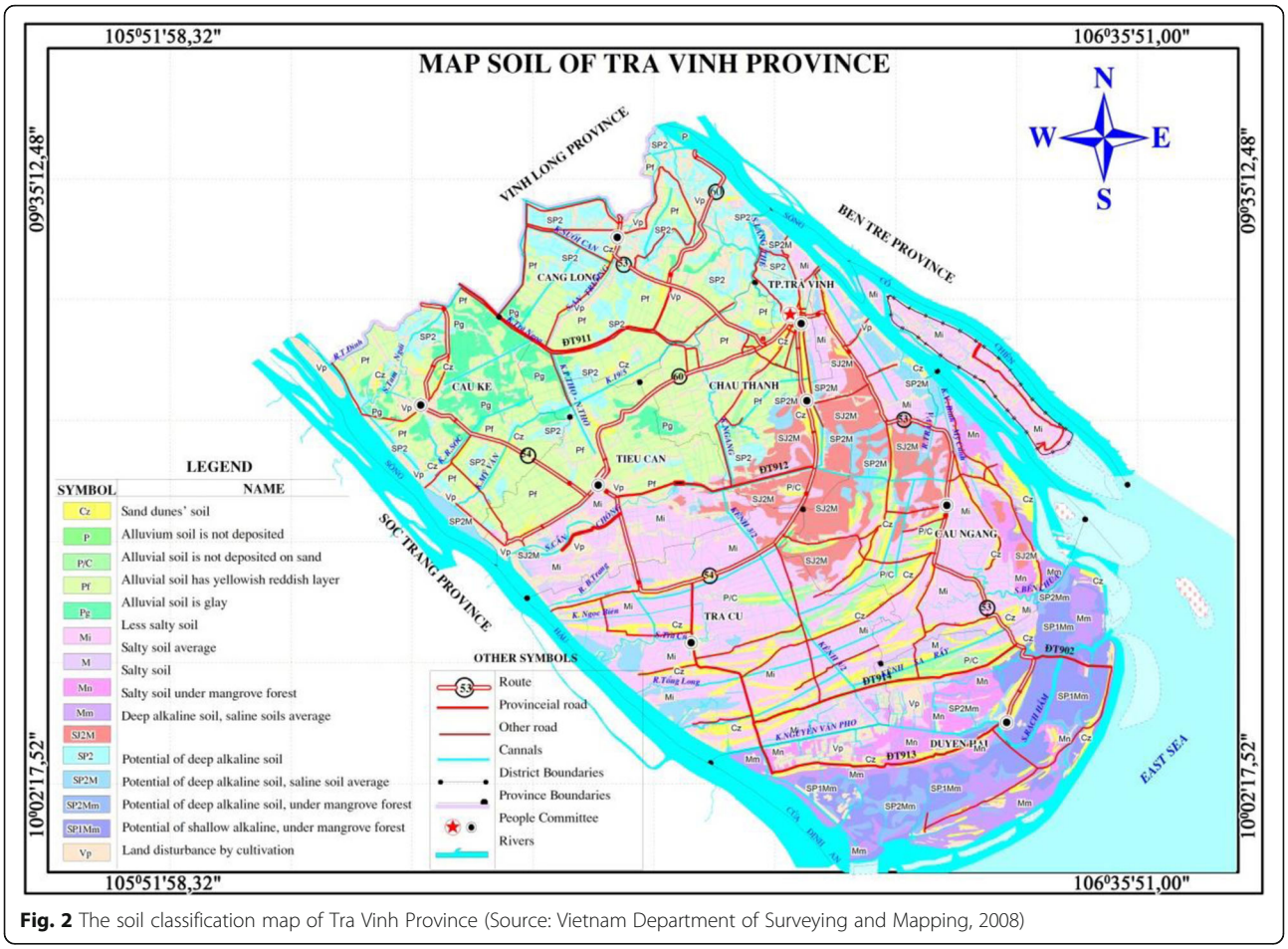

Fig. 2 The soil classification map of Tra Vinh Province (Source: Vietnam Department of Surveying and Mapping, 2008)

samples are located at different soil types, as shown in Fig. 3. The soil samples were taken in the field at different soil types on 13–14 February 2017 (i.e., during the dry season) and in weather conditions with no rainfall, but sunny (Fig. 4). Each soil sample weighs 2 kg. Sample preparation for laboratory analysis is addressed as follows: soil samples from the field must be crushed down in time, picking up the plant, gravel stone, etc., and dried in the air. The sample room must be ventilated and free of chemicals. Then, the soil samples were analyzed for quantifying $EC_{1:5}$ (Richards 1954). The electrical conductivity is measured at 25 °C from an unfiltered 1:5 soil to deionized water suspension. Soil suspensions were prepared using 35 mL of distilled water and 7 g of soil into 50 mL plastic centrifuge tubes (Cat. No. 06-443-20, Fisherbrand). Soil suspensions were continuously shaken by using a mechanical shaker (132 rpm) at 25 °C for 60 min to dissolve soluble salts. $EC_{1:5}$ is defined as the first of three steps to estimate soil salinity (ECe). It was determined by mixing 1 part soil with 5 parts distilled or deionized water. After mixing the sample and allowing the sediment to settle, the electrical conductivity of the solution was tested (Slinger and Tension 2005). Therefore, after 15 min settling time, EC was determined using a conductivity probe (Conductivity Meter SCM 902A, Apel Instrument). The EC meter was calibrated by KCl standard solution (1.413 dS/m) (Cat. No. 2974326, Hach Company, Loveland, CO, USA) prior to soil suspensions measurement. Among 41 samples, 29 samples were used for training and 12 samples for validation. The samples used for training and validation have to meet the condition of being representative for typical land use types in the regions of concern with evenly spatial distributed over the Province (Table 4 in Appendix).

(3) Land use map: The study collected land use map of Tra Vinh Province with scale of 1/100000 in 2016. The coordinate system is WGS-84 zone 48.

(4) Map of saline soil classification in Tra Vinh Province: the study collected a saline soil classification map of Tra Vinh Province with scale of 1/100000. The coordinate system is WGS-84 zone 48.

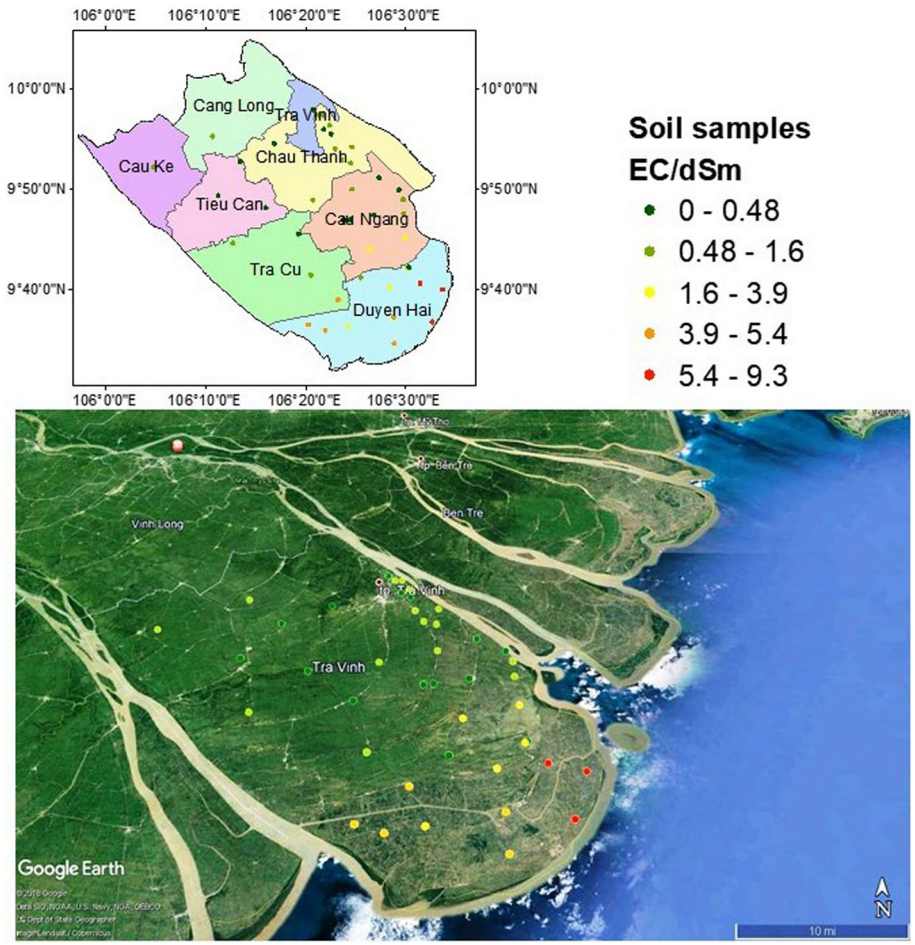

Fig. 3 Spatial distribution of soil samples and their measured $EC_{1:5}$ over Tra Vinh Province overlaid on Google Earth image

Research method

This section presents the processing steps of Landsat 8 image to map soil salinity and the method to assess soil salinity from soil samples (Fig. 5). Firstly, in order to remove the atmospheric effects, the FLAASH model was applied (Kaufman et al. 1997; Abbas and Felde et al, 2003 Khan et al. 2005 Khan 2007). Then, further steps to process Landsat 8 images include image morphology, conversion from digital number to reflectance value, cloud filtering Zanter et al, 2016, and image enhancement. Subsequently, spatial analysis tools in ArcGIS 10.3 software were used to compute indices and analyze the indices. The indices are described in Table 2. Excel software was used for normalization of the indices. Secondly, 29 samples of $EC_{1:5}$ data (Table 4 in Appendix) were analyzed with the spectral reflectance of the Landsat 8 OLI image. The soil salinity is estimated by the $EC_{1:5}$ of the soil as measured in the laboratory. Based on the results, the analysis is made to determine the relationship between reflectance values and indices of soil salinity to estimate the soil salinity from the Landsat 8 image. Various soil types reflect solar radiation differently. The difference in reflectance allows one to determine the soil type at the surface layer. Validation samples were taken from different land use/land cover types, including paddy rice field, shrimp ponds, bare land, and cropland. The sample locations are selected at different salinity intrusion degrees.

Results

Relationship between $EC_{1:5}$ and spectral reflectance bands

The relationships between $EC_{1:5}$ and spectral reflectance of Landsat 8 OLI channels are shown in Fig. 6. Thereby, salinity links to NIR and SWIR1 spectral channels, in which the NIR channel has the highest correlation with salinity. The correlation coefficient is 0.80 between $EC_{1:5}$ (ds/m) and NIR channel (Fig. 6d). Other channels from the Landsat 8 image show unclear association with soil salinity.

Fig. 4 Four photos show soil samples taken at different soil types on 13 February 2017 under sunshine condition. Detail characteristics of each point are described as follows: **a** MP01 is paddy rice field after harvest with 6 m elevation; ,**b** L11 is of former use for aquaculture for shrimp at 5 m elevation; **c** MP05 is land use to grow banana surrounded by paddy field at 5 m elevation; and **d** P9 is paddy rice field at harvest time at 3 m elevation

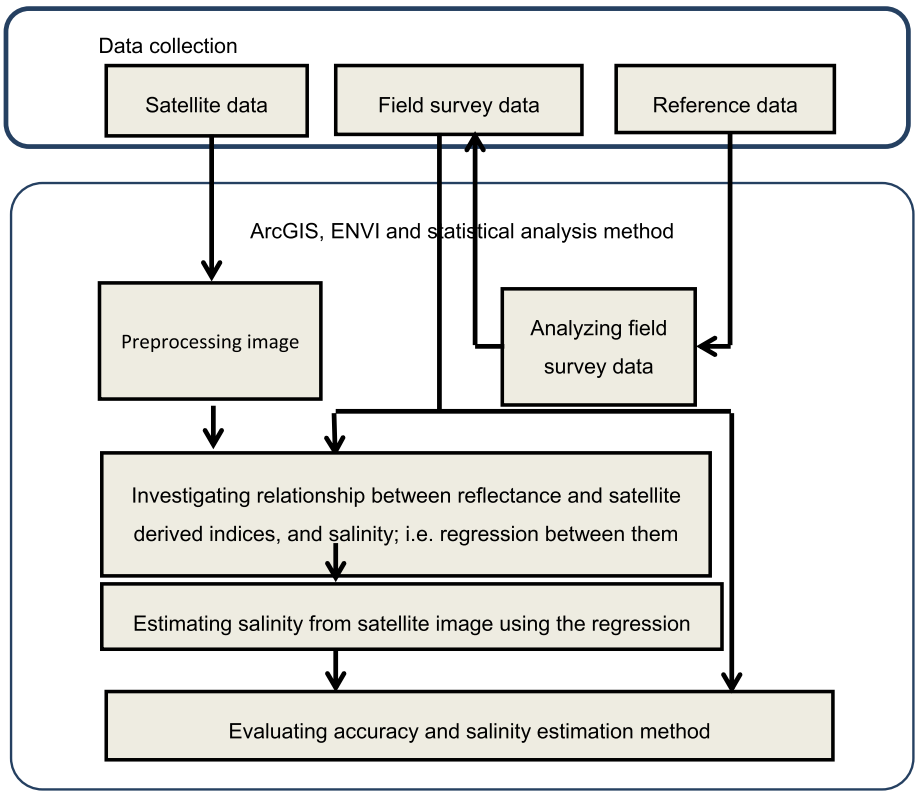

Fig. 5 The workflow of salinity retrieval using Landsat 8 OLI image

Table 2 The formulas used to derive the indices, and their references

No.	Indices	Formula	Sources
1	Salinity index - SI1	SI1 = sqrt(green^2 + red^2)	Douaoui et al. (2006)
2	Salinity index - SI2	SI2 = sqrt(green × red)	Douaoui et al. (2006)
3	Salinity index - SI3	SI3 = sqrt(blue × red)	Khan et al. (2001)
4	Salinity index - SI4	SI4 = (red × NIR)/green	Abbas and Khan (2001)
5	Salinity index - SI5	SI5 = blue/red	Abbas and Khan (2001)
6	Normalized Difference Salinity Index (NDSI)	NDSI = (red − NIR)/(red + NIR)	Khan et al. (2001)
7	Normalized Difference Vegetation Index (NDVI)	NDVI = (NIR − red)/(red + NIR)	Khan et al. (2001)
8	Soil Adjusted Vegetation Index (SAVI) (L = 0.5)	SAVI = (1 + L) × NIR − red/L + NIR + red	Alhammadi and Glenn (2008)
9	Vegetation Soil Salinity Index (VSSI)	VSSI = 2 × green − 5 × (red + NIR)	Dehni and Lounis (2015)

Figure 7 shows a great difference between red, green, blue, NIR, and SWIR1 spectral channels corresponding to the strong reflective zones of the plants. The soil types with low salinity correspond to high vegetation areas that exhibit high NIR values. The red, green, blue, and SWIR1 channels show different reflections for different salinity types, but with less reflectance for the NIR channel. Therefore, the NIR channel can be used to derive reliable results in salt estimation. Different salt thresholds will receive different reflectivity curves, which will serve as a basis for selecting the estimation model.

Relationship between $EC_{1:5}$ and indices derived from Landsat data

We also investigate the relationship between $EC_{1:5}$ and remote sensing indices as shown in Fig. 8. The indices are described in Table 2.

From the scatter plots in Fig. 8, it shows that the SI1, SI2, SI3, and SI5 indices are weakly correlated with the salinity. In contrast, the SI4, NDSI, NDVI, SAVI, and VSSI have a clear relationship with the salinity with coefficient of determination (r^2) higher than 0.41.

The salinity estimation and validation

After using the regression method for five indices derived from Landsat data including SI4, NDVI, NDSI, SAVI, VSSI, and NIR for the soil salinity, it is found that the regression models have a well-defined coefficient (R^2) between salty value obtained from the field measurement and salty values derived from remote sensing data. The highest coefficient is 0.80 between $EC_{1:5}$ and NIR channel reflectance as shown in Table 3. Table 3 reviews the regression models for estimating EC from remote sensing data, characterized by various indices including NIR, SI4, NDSI, NDVI, SAVI, and VSSI. It also presents R^2, P value, and standard errors of EC (dS/m).

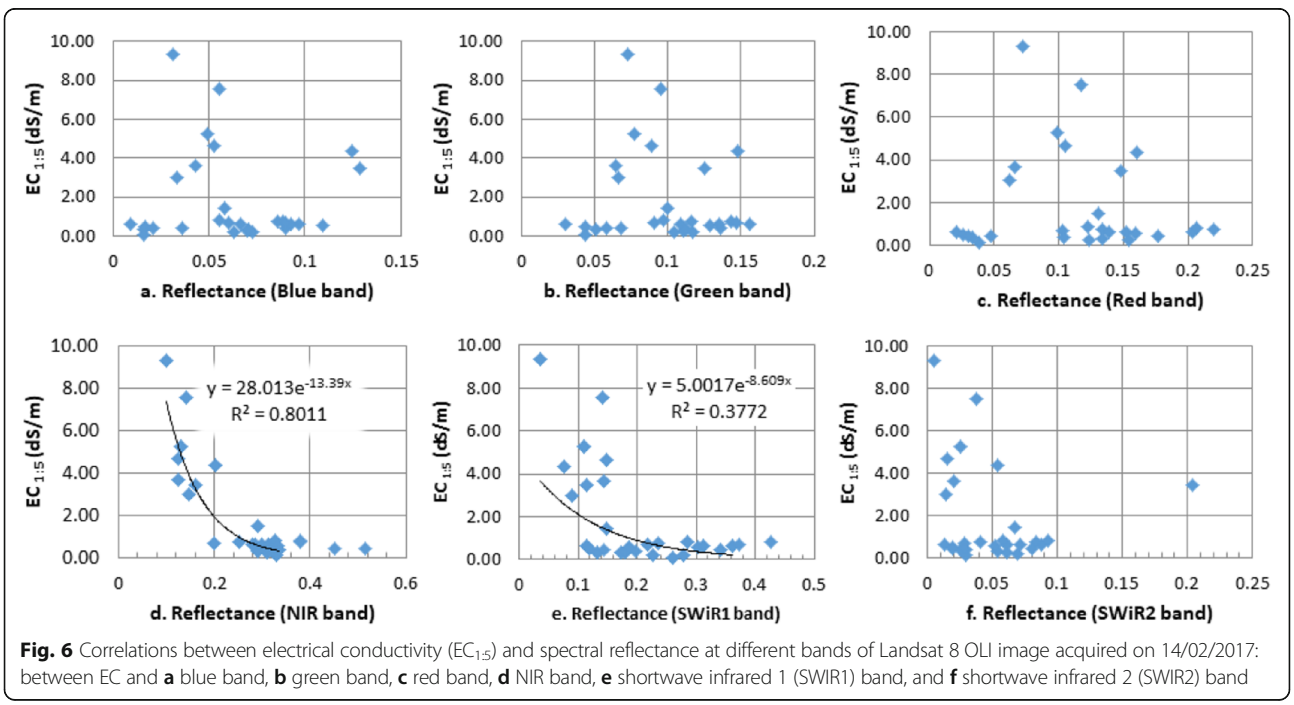

Fig. 6 Correlations between electrical conductivity ($EC_{1:5}$) and spectral reflectance at different bands of Landsat 8 OLI image acquired on 14/02/2017: between EC and **a** blue band, **b** green band, **c** red band, **d** NIR band, **e** shortwave infrared 1 (SWIR1) band, and **f** shortwave infrared 2 (SWIR2) band

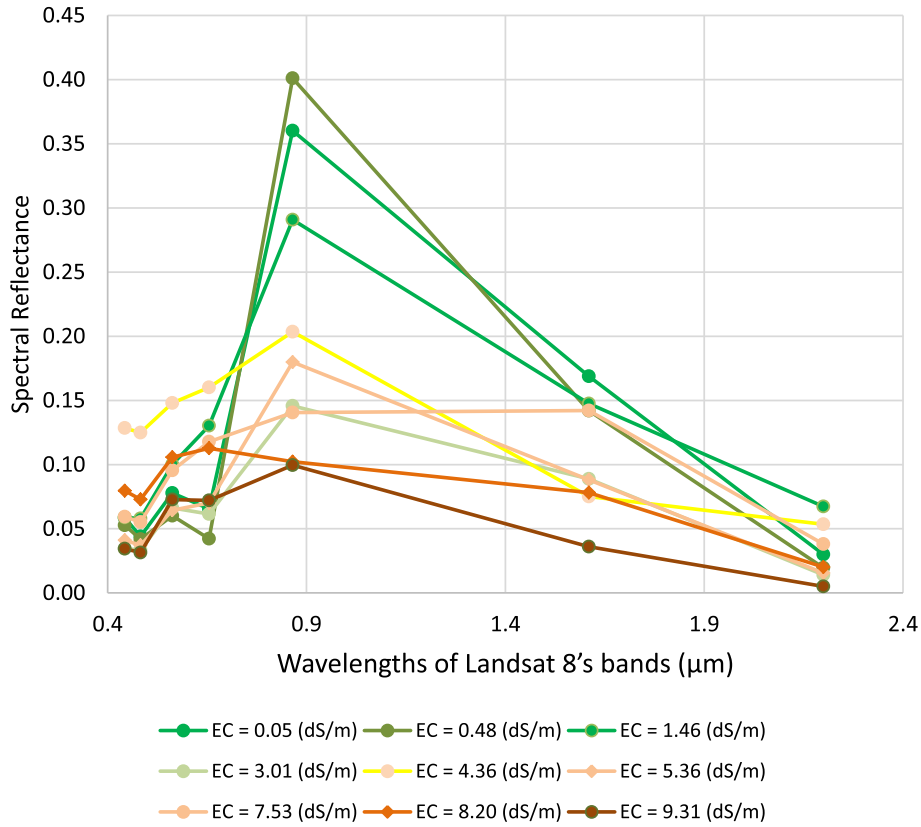

Fig. 7 Spectral reflectance profiles of the major salt-affected lands extracted from Landsat 8 image in the Tra Vinh Province

Estimation of soil salinity and accuracy assessment

Accuracy assessment

The statistical analysis results are shown in Table 3. All of six regression models have a high statistical coefficient (R^2) with P value less than 0.05. Therefore, the study adopts all of these models to estimate the salinity of soil based on the remote sensing indices for the 12 validation samples (Table 4 in Appendix). Figure 9 shows that there is a strong correlation between estimated $EC_{1:5}$ and observed $EC_{1:5}$ when using the first and sixth models. It is found that the correlation between $EC_{1:5}$ and NIR and between $EC_{1:5}$ and VSSI model are 0.89 and 0.77, respectively, and the corresponding lowest gradient values (bias) are 0.38 and 0.28, respectively, indicating that the two models were the most suitable ones while comparing with the salinity values.

Results of estimated salinity mapping

Accuracy assessment indicates that salinity ($EC_{1:5}$, dS/m) shows its high correlation with NIR and VSSI indices. Therefore, this study generates salinity maps for the entire Tra Vinh Province using the NIR model (Fig. 10) and VSSI model (Fig. 11). Soil salinity is classified into five levels based on Chhabra (1996) and Skaggs et al. (2014).

Discussion

Tra Vinh is characterized by lowland and located in the coastal plain of downstream Mekong River so that it is seriously affected by tides and sea level rising. Seawater intrudes into the inland through the river when high tide occurs or sea dikes were broken by storms. Salt water can also be followed by capillaries, cracks in the soil, to penetrate deep into the interior through the sea dikes. This is the main mechanism of the salinization process in Tra Vinh Province. The purpose of this study is to map the spatial distribution of soil salinity to assist management and agricultural planning. Hence, if the samples were taken at a depth of less than 5 cm corresponding to most of the root zone of the plants where the topsoil layers only show the organic part of the roots. This topsoil is of a plowed area, raised for cultivation with fertilizer, lime, organic residue, and other chemicals. Therefore, the samples at a depth less than 5 cm have limitation to identify the content of natural salty in the soils.

In agricultural irrigation, salts are not absorbed at the surface, instead of that salts are accumulated in the

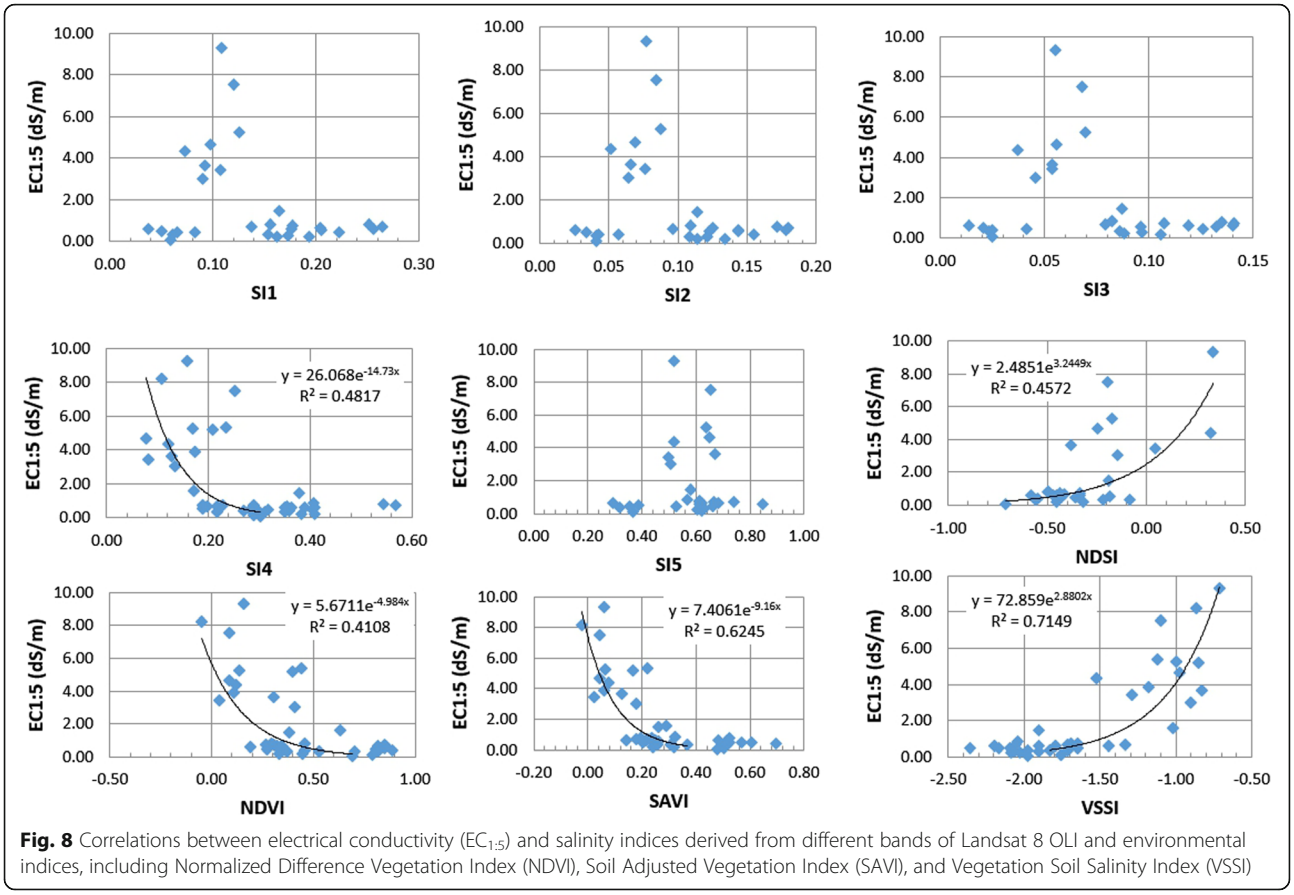

Fig. 8 Correlations between electrical conductivity ($EC_{1:5}$) and salinity indices derived from different bands of Landsat 8 OLI and environmental indices, including Normalized Difference Vegetation Index (NDVI), Soil Adjusted Vegetation Index (SAVI), and Vegetation Soil Salinity Index (VSSI)

lower portion of the root-zone (Mougenot et al. 1993). When salinity does exist at the surface, it can be successfully detected with remote sensing techniques, but only very saline soils, where the influence on vegetation is minimal (Mulla et al. 2013). In general, when the plants experience biotic and abiotic stress (including salinity), their photosynthetic activity decreases, causing increased visible reflectance and reduced NIR reflectance from the vegetation (U. S. Salinity Laboratory Staff 1954). Essentially, this study intended to determine the indirect relationship between the salinity of the topsoil and spectral reflectance by measurement methods and to determine the actual salinity from the samples at the depth of 20 cm.

According to FAO (1976), saline soil is defined as amount of salt in ECe > 4mmho/cm (ECe is EC measured by saturation extraction method). This is the definition only concerning the amount of salt that presents in the soil, without considering the other chemical properties. The U.S. Salinity Laboratory (U.S. Salinity Laboratory Staff 1954) classifies agricultural soil salinities as 0–2 dS/m = non-saline; 2–4 dS/m = slightly saline; 4–8 dS/m = moderately saline; 8–16 dS/m = strongly saline; and > 16 dS/m = extremely saline, where salinity is quantified as the

Table 3 Regression models for estimating EC from remote sensing data

No.	Regression formula	R^2	*P* value	Standard error of EC (dS/m)
1	$EC_{1:5} = 28.013 \times e^{-13.39 \times NIR}$	0.80	2.71E−08	1.29
2	$EC_{1:5} = 26.068 \times e^{-14.73 \times SI4}$	0.48	0.00761	2.44
3	$EC_{1:5} = 2.485 \times e^{3.2449 \times NDSI}$	0.46	0.00019	1.88
4	$EC_{1:5} = 5.671 \times e^{-4.984 \times NDVI}$	0.41	0.00034	2.15
5	$EC_{1:5} = 7.406 \times e^{-9.16 \times SAVI}$	0.62	3.78E−07	1.69
6	$EC_{1:5} = 72.86 \times e^{2.8802 \times VSSI}$	0.71	1.39E−05	1.76

Appendix

Table 4 Salinity information of 41 samples, among which 29 (~ 70%) samples are used for training and 12 (~ 30%) samples highlighted in gray color are used for validation

No.	Code	X (UTM WGS84_Zone48) (m)	Y (UTM WGS84_Zone48) (m)	Electrical conductivity (d/Sm)	Elevation (meter)	Soil types
1	L.01	649531	1098282	0.05	0	Sand dunes' soil
2	P4N	654372	1081554	0.10	0	Sand dunes' soil
3	P5N	653173	1081562	0.21	0	Less salty soil
4	P8	659690	1089314	0.22	0	Less salty soil
5	MP06	634243	1092238	0.30	6	Alluvial soil has yellowish reddish layer
6	MP01	650832	1097403	0.31	6	Less salty soil
7	MP05	640473	1095595	0.35	5	Alluvial soil has yellowish reddish layer
8	P2N	656426	1070927	0.36	0	Salty soil average
9	P7N	658718	1082446	0.37	0	Sand dunes' soil
10	MP13	644985	1078898	0.42	2	Less salty soil
11	MP08	630202	1085956	0.45	2	Alluvial soil has yellowish reddish layer
12	P5N2	653218	1081402	0.45	0	Less salty soil
13	MP11	638932	1083668	0.48	3	Less salty soil
14	L.02	651590	1094664	0.51	3	Deep alkaline soils, saline soil average
15	MP02	650585	1099018	0.57	3	Less salty soil
16	P9-2	664137	1085331	0.60	0	Salty soil average
17	MP10	632954	1077177	0.62	3	Less salty soil
18	P10	664207	1082773	0.62	0	Salty soil
19	L.06	652801	1092571	0.63	3	Deep alkaline soils, saline soil average
20	MP03	649479	1100892	0.64	3	Less salty soil
21	P2N2	656415	1070929	0.64	0	Salty soil average
22	MP07	629148	1096882	0.69	1	Alluvial soil has yellowish reddish layer
23	MP14	647257	1071374	0.73	1	Salty soil under mangrove forest
24	MP04	648527	1100904	0.75	4	Less salty soil
25	L.03	651590	1094664	0.75	3	Deep alkaline soils, saline soil average
26	L.05	654466	1092021	0.80	3	Less salty soil
27	L.04	654689	1095002	0.83	3	Potential of deep alkaline soil, saline soil average
28	P9	664121	1085370	1.46		Soil disturbance by cultivation
29	L.07	654726	1087204	1.60		Sand dunes' soil
30	P3N	657943	1076231	3.01		Less salty soil
31	L.13	654128	1061941	3.45		Salty soil
32	P12	661696	1069167	3.65		Salty soil
33	L11N	664955	1072706	3.88		Salty soil average
34	P13	652229	1066825	4.36		Less salty soil
35	L.12	662432	1063649	4.66		Salty soil
36	L.14	649923	1061131	5.19		Salty soil under mangrove forest
37	L.11	662631	1058792	5.26		Soil disturbance by cultivation
38	L.15	646814	1062193	5.36		Soil disturbance by cultivation
39	L.10	669545	1062763	7.53		Potential of shallow alkaline soil, under mangrove forest
40	L.08	667320	1069881	8.20		Potential of shallow alkaline soil, under mangrove forest
41	L.09	671460	1068779	9.31		Potential of shallow alkaline soil, under mangrove forest

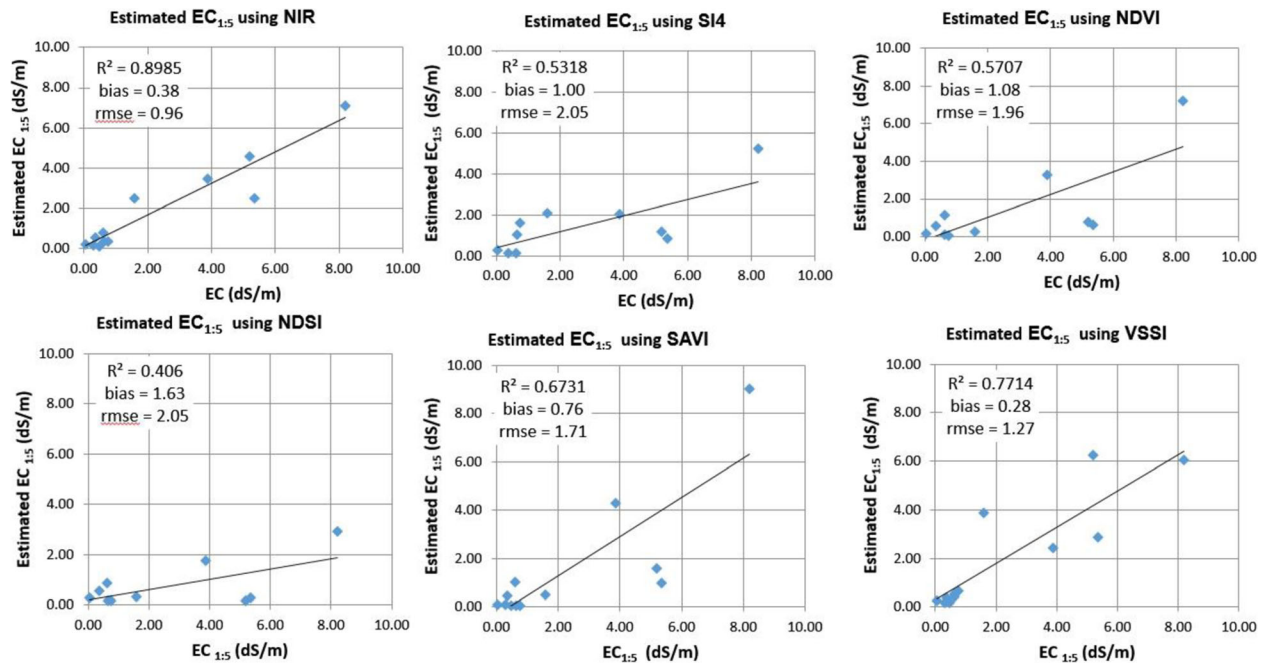

Fig. 9 Correlation of $EC_{1:5}$ derived from Landsat 8 OLI and observed $EC_{1:5}$ from field survey data for the 12 test samples over Tra Vinh Province

electrical conductivity of a saturated soil paste extract (ECe with units of dS/m). At ECe < 20 dS/m, the ability to directly assess soil salinity from bar soil reflectance is limited (He et al. 1992; Metternicht and Zinck 2003; Allbed and Kumar 2013) He et al. (2012) Metternicht & Zinck. (2012).

According to He et al. (1992), electrical conductivity ($EC_{1:5}$) of a soil extract is the most widely used parameter for describing soil salinity (Rayment and Higginson 1992). Electrical conductivity is estimated by the concentration of ions in the soil that predominantly consists of the cations Na+, Ca^{2+}, K^{+}, and Mg^{2+} and the anions Cl^{-}, SO_4^{2-} and HCO_3^{-} (Rhoades et al. 1989; Sumner and Naidu 1998). In soil, ions present mainly in soil solution and are adsorbed in soil colloids. The standard laboratory method for determining the $EC_{1:5}$ of a soil is by using a saturated paste extract (ECe) (Rayment and Higginson 1992). Due to the difficulties encountered in determining the appropriate water saturation point when preparing a saturated paste extract (Hogg and Henry 1984), soil to water ratios of 1:1, 1:2, 1:2.5, 1:5, and 1:10 have been used to determine the $EC_{1:5}$ values of soils (Slavich and Petterson 1993; Franzen 2007; Sonmez et al. 2008; Rayment & Lyons, 2011; Wang et al. 2011).

The 1:5 ratio has the advantages of simplicity and reduced time and cost as compared to saturation paste extracts (Reitemeier 1946) and also dissolves larger amount of solutes than the saturation paste extracts, especially for sparingly soluble salts (Metternicht Zinck 2003). Therefore, this study has chosen the $EC_{1:5}$ index to determine the soil salinity. The soil salinity map with five salty levels serves for land management and agricultural planning. Remote sensing technology has been proven its efficiency in the investigation of soil salinity on a large area. Results show that using Landsat image 8 OLI images allows one to extract and monitor the features of the salty land. They indicate that the salinity of the soil has strong relationship with the reflectance at NIR channel. This is in line with the results of research presented by Elnaggar and Noller (2009). However, the SWIR channel does not have a high correlation with $EC_{1:5}$, which has been found in the study (Csillag 1993), reflecting higher values of the visible and infrared channels near the surface of non-salty soils. The relationship is unclear for the sand patterns with a high salinity value and low reflectance in the NIR channel. This may be due to the influence of the naturally hot dry climate conditions of the area of research, such as Saudi Arabia in the Middle East. He et al. (1992) found a strong relationship between the SI and salinity indicator in the red channel, which has a high correlation with EC. A similar result is seen in the study by Noroozi et al. (2012). In the case of Tra Vinh Province, it is affected by salt brought from the sea by the tide and rising sea levels. For this reason, the areas

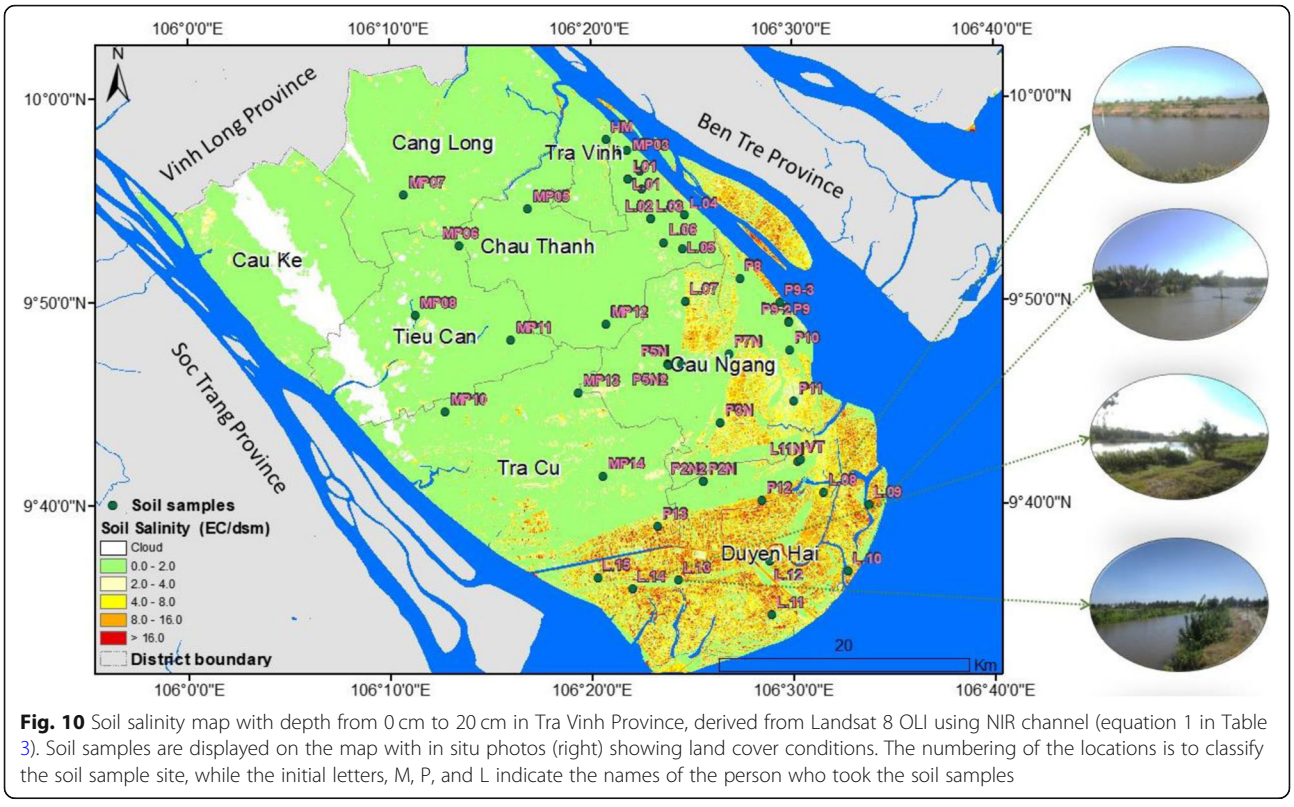

Fig. 10 Soil salinity map with depth from 0 cm to 20 cm in Tra Vinh Province, derived from Landsat 8 OLI using NIR channel (equation 1 in Table 3). Soil samples are displayed on the map with in situ photos (right) showing land cover conditions. The numbering of the locations is to classify the soil sample site, while the initial letters, M, P, and L indicate the names of the person who took the soil samples

contaminated by salt due to low elevation and flooded by tide flow exhibited lower reflectance on the NIR channel in comparison with those of the other regions.

Results of the evaluation model to estimate soil salinity by using NIR channel show the signatures of salinity dynamics in the research area. They were validated with simultaneous field data with coefficient of determination, R^2 = 0.89 and RMSE = 0.96 dS/m. The same was found for the VSSI index, with R^2 = 0.77 and RMSE = 1.27 dS/m. This shows that the NIR channel and VSSI index are suitable for soil salinity estimation (Fig. 8 and Fig. 9). However, the underestimation is common in existing remote sensing studies. For this case, the underestimates are increased with the degree of soil salinization. The major contribution for the underestimation may result from the data inaccuracy other than model ineffectiveness. Bias analysis confirmed that improper atmospheric correction contributed to underestimation or field sampling representativeness within remote sensing pixels was probably the major cause for the underestimation. Notably, despite of this limitation, this research achieved a reasonably good performance in retrieving soil salinity from new-generation multi-spectral sensors. This has been done in the various studies by using environmental indicators. By taking for example the SI, NDVI, NDMI, and NDSI derived from Landsat satellite images to study environmental conditions (Abdul-Qadir and Benni 2010), it has been proven of the high potential in enhancement and extraction of soil salinity from remote sensing data. Results of this study indicate that the NIR channel demonstrates a higher potential to detect the salinity intrusion in the Mekong Delta with a higher degree of confidence. Our findings match with outcomes of Allbed and Kumar (2013) in that the information on the salinity of the soil can be found in the NIR and SWIR channels. Allbed and Kumar (2013) found that the Red channel in the series Landsat ETM+ images has a high correlation with $EC_{1:5}$ for Iraq. In the future, there is a need to extend the research scope based on long-term spatiotemporal monitoring of soil salinity to have a better understanding of interaction between natural conditions (soil moisture, soil type, natural salt content, etc.) and human impacts (irrigation, land use, etc.). These nature and human interaction should result in soil contamination as it can be observed by using spectral reflectance of the remote sensing images. This is very valuable for agricultural soil salinity mapping worldwide especially in the developing countries since this method is of low cost and acceptable accuracy.

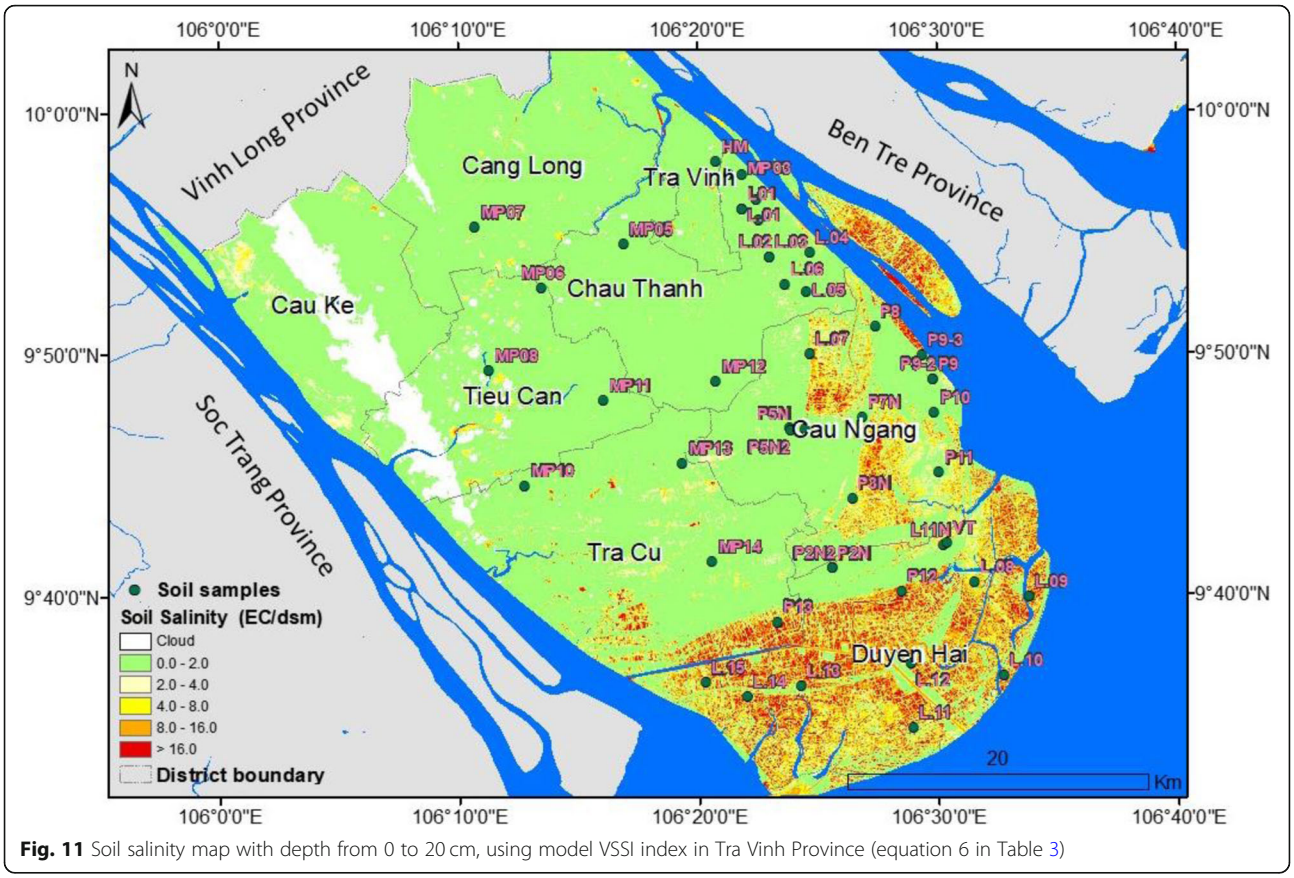

Fig. 11 Soil salinity map with depth from 0 to 20 cm, using model VSSI index in Tra Vinh Province (equation 6 in Table 3)

Conclusions

This study investigates salinity intrusion in Tra Vinh Province, which is the most affected place among seven coastal provinces in the Mekong Delta. A method of spatially monitoring soil salinity is proposed by using satellite data-derived variables in order to support the management of land resources and to determine the suitable crops to cultivate. Results of the study show that use of Landsat 8 OLI images allows one to estimate the salinity value of the soil surface with an acceptable accuracy. It is found that the values of NIR band and VSSI indices are highly correlated with $EC_{1:5}$ (dS/m) with coefficient of determinations 0.89 and 0.77, respectively, with corresponding lowest gradient values (biases) of 0.38 and 0.28, respectively. Error analysis showed that soil salinity was relatively accurate for low saline soils and underestimated for highly saline soils. The underestimation may result from the poor representativeness of soil samples. That is to say, the NIR and VSSI models' results most fit the observed salinity values in comparison with the other models implemented in our study. It is inevitable that climate change is affecting Tra Vinh Province by manifesting the sea level rise, salt water intrusion, and drought that lead to increased soil salinity in the study areas, especially in the lower-elevation terrains, such as coastal areas and estuaries. As a result, the agricultural cultivation in Tra Vinh Province will be altered. Proper measures to mitigate the impacts of increased soil salinity must be designed in order to sustain the agriculture and economic development of Tra Vinh Province.

In addition, there is a need to further develop and improve the skills in the monitoring and forecasting of salinization in the agricultural areas of Tra Vinh Province and neighboring regions with potential to be vulnerable to salinity intrusion. For example, adopting a newly developed normalized difference latent heat index (NDLI) that could enhance the sensitivity on surface water availability over land surface may lead to an improved monitoring of the salinization (Liou et al. 2019). Furthermore, although the proposed methodology of the study has been demonstrated to perform well in terms of extracting soil salinity information by using the Landsat OLI data, an improved version of the proposed methodology especially in spatial domains will be even more beneficial to achieve a greater efficiency in contributing to the orientation and planning of agricultural production areas of the salinity intrusion vulnerable regions.

Nevertheless, the current version of the proposed methodology is ready to be applied to the other coastal provinces of the Mekong Delta in order to assess the terrains' vulnerability at a regional scale with low cost and acceptable accuracy for the planning of land use.

Acknowledgements
The authors appreciate the United States Geological Survey (USGS) for providing the satellite data used in this study.

Authors' contributions
Conceptualization was done by HPT and KAN. Data curation was done by HPT, PPH, and THN. Formal analysis was done by KAN. Funding acquisition was done by YAL and THN. Investigation was done by HPT and PPH. Methodology was done by HPT. Project administration was done by HPT. Supervision was done by KAN and YAL. Writing of the original draft and reviewing, editing, revising, and finalization of the manuscript was done by YAL. All authors read and approved the final manuscript.

Funding
This research was financially supported by the VAST under the code VAST05.04/16-17 and MOST of Vietnam under code KHCN_TNB/14-19/C23 and partially supported by MOST of Taiwan under the codes 107-2111-M-008-036 and 105-2221-E-008-056-MY3.

Availability of data and materials
Please contact authors for the data supporting this study.

Competing interests
The authors declare that they have no competing interests.

Author details
[1]Center for Space and Remote Sensing Research, National Central University, No. 300, Jhongda Rd., Jhongli District, Taoyuan City 32001, Taiwan, Republic of China. [2]Institute of Geography, Vietnam Academy of Science and Technology (VAST), No.18 Hoang Quoc Viet Rd., Cau Giay Dist.,, Hanoi City, Vietnam. [3]Graduate University of Science and Technology, VAST, No. 18 Hoang Quoc Viet Rd., Cau Giay Dist.,, Hanoi City, Vietnam. [4]Ho Chi Minh City Institute of Resources Geography, VAST, No. 1, Mac Dinh Chi St., 1st District, Ho Chi Minh City, Vietnam. [5]Ho Chi Minh City Space Technology Application Center, Vietnam National Space Center, VAST, Ho Chi Minh City, Vietnam. [6]Representative Office of VAST in Ho Chi Minh City, Ho Chi Minh City, Vietnam.

Received: 26 June 2019 Accepted: 1 November 2019
Published online: 06 January 2020

References

Abbas A, Khan S (2007) Using remote sensing techniques for appraisal of irrigated soil salinity. In: Oxley, L. and Kulasiri, D., Eds., MODSIM 2007 International Congress on Modelling and Simulation, Modelling and Simulation Society of Australia and New Zealand, 2632-2638.
Abdul-Qadir AM, Benni TJ (2010) Monitoring and evaluation of soil salinity term of spectral response using Landsat images and GIS in Mesopotamian plain Iraq J. Desert Stud. 2:19–32
Aldakheel YY (2011) Assessing NDVI spatial pattern as related to irrigation and soil salinity management in Al-Hassa Oasis. Saudi Arabia. J. Indian Soc. Remote 39:171–180
Alhammadi M.S, Glenn, E.P (2008) Detecting date palm trees health and vegetation greenness change on the eastern coast of the United Arab Emirates using SAVI, Int. J. Remote Sens., 2008; vol. 29, no. 6: 1745–1765.
Allbed A, Kumar L (2013) Soil salinity mapping and monitoring in arid and semi-arid regions using remote sensing technology: a review. Advances in Remote Sensing 2:373–385
Allbed A, Kumar L, Aldakheel YY (2014) Assessing soil salinity using soil salinity and vegetation indices derived from IKONOS high-spatial resolution imageries: applications in a date palm dominated region. Geoderma 230–231:1–8
CGIAR Research Centers in Southeast Asia (2016). The drought and salinity intrusion in the Mekong River Delta of Vietnam. Assessment Report. 25-28 April, Ben Tre, Tra Vinh, Kien Giang, Vietnam.
Chhabra R (1996) Soil salinity and water quality. Balkema, Rotterdam, The Netherlands
Csillag F, Pásztor L, Biehl LL (1993) Spectral band selection for the characterization of salinity status of soils. Remote Sens. Environ 43(3):231–242
Dehni A, Lounis M (2012). Remote sensing techniques for salt affected soil mapping: application to the Oran region of Algeria, Procedia Eng., 2012; vol. 33: 188–198.
Douaoui AEK, Nicolas H, Walter C (2006) Detecting salinity hazards within a semiarid context by means of combining soil and remote-sensing data. Geoderma 134:217–230
Dwivedi RS, Rao BRM (1992) The selection of the best possible Landsat TM band combination for delineating salt-affected soils. Int. J. Remote Sens. 13:2051–2058
Dwivedi RS, Sreenivas K (1998) Image transforms as a tool for the study of soil salinity and 33 alkalinity dynamics. Int. J. Remote Sens. 19:605–619
Elnaggar AA, Noller JS (2010) Application of remote-sensing data and decision-tree analysis to mapping salt-affected soils over large areas. Remote Sens. 2: 151–165
Fan X, Liu Y, Tao J, Weng Y (2015) Soil salinity retrieval from advanced multi-spectral sensor with partial least square regression. Remote Sens. 7:488–511
Farifteh J, van der Meer FD, Atzberger C (2007) Carranza, E.J.M. Quantitative analysis of salt-affected soil reflectance spectra: a comparison of two adaptive methods (PLSR and ANN). Remote Sens. Environ. 110:59–78
Felde GW, Anderson G P, Adler-Golden S M, Matthew MW, A. Berk (2003) Analysis of Hyperion data with the FLAASH atmospheric correction algorithm. Algorithms and Technologies for Multispectral, Hyperspectral, and Ultraspectral Imagery IX. SPIE Aerosense Conference, Orlando, 21–25 April.
Fernandez-Buces N, Siebe C, Cram S, Palacio JL (2006) Mapping soil salinity using a combined spectral response index for bare soil and vegetation: a case study in the former lake Texcoco. Mexico. J. Arid Environ. 65:644–667
Franzen D (2007) Managing saline soils in North Dakota Available online at http:// www.ag.ndsu.edu/pubs/plantsci/soilfert/sf1087-1.htm.
Goldshleger N, Livne I, Chudnovsky A, Ben-Dor E (2012) New results in integrating passive and active remote sensing methods to assess soil salinity: a case study from Jezre'el Valley. Israel. Soil Sci. 177:392–401
Gorji T, Sertel E, Tanik A (2017) Monitoring soil salinity via remote sensing technology under data scarce conditions: a case study from Turkey. Ecological Indicators 74:384–391. https://doi.org/10.1016/j.ecolind.2016.11.043 http://vro.agriculture.vic.gov.au/dpi/vro/vrosite.nsf/pages/water_spotting_soil_salting_class_ranges
He H, Roach RR, and Hoseney RC (1992) Effect of nonchaotropic salts on flour bread-making properties. Cereal Chem. 69:366–71.
He Y, DeSutter T, Prunty L, Hopkins D, Xinhua J, Wysocki DA (2012) Geoderma 185 – 186 (2012) 12 – 17. 85. Rayment, G.E. and Higginson, F.R. Australian laboratory handbook for soil and water chemical methods. Inkata Press. Melbourne.
Hogg TJ, Henry JL (1984) Comparison of 1:1 and 1:2 suspensions and extracts with the saturation extracts in estimating salinity in Saskatchewan. Canadian J Soil Sci 64:699–704
Ivits E, Cherlet M, Tóth T, Lewinska K, Tóth G (2013) Characterisation of productivity limitation of salt-affected lands in different climatic regions of Europe using remote sensing derived productivity indicators. Land Degradation and Development 24:438–452
Kaufman Y J, Wald A. E, Remer L A, Gao B C, Li R R, Flynn L (1997) The MODIS 2.1-mm channel-correlation with visible reflectance for use in remote sensing of aerosol. IEEE Transactions on Geoscience and Remote Sensing. Vol. 35: 1286-1298.
Khan NM, Rastoskuev VV, Sato Y, Shiozawa S (2005) Assessment of hydrosaline land degradation by using a simple approach of remote sensing indicators, Agric. Water Manag., vol. 77: 96–109.
Khan NM, Rastoskuev VV, Shalina EV, Sato Y (2001) Mapping salt-affected soils using remote sensing indicators - a simple approach with the use of GIS IDRISI. Ratio. 5–9
Liou YA, Le MS, Chien H (2019) Normalized difference latent heat index for remote sensing of land surface energy fluxes. IEEE Trans Geosci Remote Sens 57(3):1423–1433. https://doi.org/10.1109/TGRS.2018.2866555
Liou YA, Nguyen KA, Li MH (2017) Assessing spatiotemporal eco-environmental vulnerability by Landsat data. Ecological Indicators 80:52–65. https://doi.org/10.1016/j.ecolind.2017.04.055
Madani AA (2005) Soil salinity detection and monitoring using Landsat data: a case study from Siwa Oasis. Egypt. Gisci. Remote Sens 42:171–181

Metternicht G, Zinck A (2008) Remote sensing of soil salinization: impact on land management, CRC Press; ISBN 9781420065022.
Metternicht G, Zinck J (2003) Remote sensing of soil salinity: potentials and constraints. Remote Sens Environ 85:1–20. https://doi.org/10.1016/S0034-4257(02)00188-8
Mougenot B, Pouget M, Epema G. F (1993) Remote sensing of salt affected soils. Remote Sens Rev, 7: 241–259.
Mulla DJ (2013) Twenty five years of remote sensing in precision agriculture: key advances and remaining knowledge gaps. Biosyst Eng 11:358–371
Nawar S, Buddenbaum H, Hill J, Kozak J (2014) Modeling and mapping of soil salinity with reflectance spectroscopy and Landsat data using two quantitative methods (PLSR and MARS). Remote Sensing 6:10813–10834
Nguyen AD, Savenije HH, Pham DN, Tang DT (2008) Using salt intrusion measurements to determine the freshwater discharge distribution over the branches of a multi-channel estuary: the Mekong Delta case. Estuarine Coastal Shelf Sci. 77(3):433–445. https://doi.org/10.1016/j.ecss.2007.10.010
Nguyen KA, Liou YA (2019a) Global mapping of eco-environmental vulnerability from human and nature disturbances. Science of the Total Environment, 664: 995–1004, https://doi.org/10.1016/j.scitotenv.2019.01.407.
Nguyen KA, Liou YA (2019b) Mapping global eco-environment vulnerability due to human and nature disturbances. MethodsX, Vol. 6: 862-875https://doi.org/10.1016/j.mex.2019.03.023.
Nguyen KA, Liou YA, Li MH, Tran TA (2016) Zoning eco-environmental vulnerability for environmental management and protection. Ecological Indicators 69:100–117. https://doi.org/10.1016/j.ecolind.2016.03.026
Nguyen KA, Liou YA, Terry JP (2019) Vulnerability and adaptive capacity maps of Vietnam in response to typhoons. Science of the Total Environment 682:31–46. https://doi.org/10.1016/j.scitotenv.2019.04.069
Nguyen T, Tanaka H (2007) Study on the effect of morphology change on salinity distribution in the Dinh An estuary, lower Mekong River of Vietnam, J. Coastal Res., SI 50: 268– 272.
Noroozi AA, Homaee M, Farshad A (2012) Integrated application of remote sensing and spatial statistical models to the identification of soil salinity: a case study from Garmsar Plain. Iran. J. Environ. Sci. 9:59–74
Nowacki DJ, Ogston AS, Nittrouer CA, Fricke AT, Pham DTV (2015) Sediment dynamics in the lower Mekong River: transition from tidal river to estuary. J Geophys Res: Oceans, 6383-6388. https://doi.org/10.1002/2015JC010754.
Prentice V L (1972) Multispectral remote sensing techniques applied to salinity and drainage problems in the Columbia Basin, Washington, PhD Thesis, Michigan Univ., Ann Arbor. 237 p.
Provincial Report of Tra Vinh on the current state of the environment for 5 years (2011-2015). Department of Natural Resources and Environment of Tra Vinh Province, July 2015. In Vietnamese.
Rayment GE, Higginson FR (1992) Australian laboratory handbook for soil and water chemical methods. Inkata Press, Melbourne
Rayment GE, Lyons DJ (2011) Soil chemical methods-Australasia. Csiro Publishing, Collingwood, Victoria
Reitemeier RF (1946) Effect of moisture content on the dissolved and exchangeable ions of soils of arid regions. Soil Science 61:195–214
Rhoades JD, Manteghi NA, Shouse PJ, Alves WJ (1989) Estimating soil salinity from saturated soil-paste electrical conductivity. Soil Science Society of America Journal 53:428–433
Richards LA (1954) Diagnosis and improvement of saline and alkali soils. U. S. Dept. Agric. Handbook No. 60: 65-68.
Richardson AJ, Gerbermann AH, Gausman HW, Cuellar JA (1976) Detection of saline soils with Skylab Multispectral Scanner Data. Photogram Eng Remote Sens 42(5):679–684
Scudiero E, Skaggs TH, Corwin DL (2015) Regional scale soil salinity evaluation using Landsat ETM+ canopy reflectance. Remote Sens Environ 169:335–343
Seghal JL, Saxena RK, Verma KS (1988) Soil resource inventory of India using image interpretation techniques, Remote Sensing Is a Tool for Soil Scientists, Proceeding of the 5th Symposium of the Working Group Remote Sensing ISSS. Budapest, Hungary, pp 17–31
Setia R, Lewis M, Marschner P, Raja Segaran R, Summers D, Chittleborough D (2013) Severity of salinity accurately detected and classified on a paddock scale with high resolution multispectral satellite imagery. Land Degrad. Dev. 24:375–384
Shammi M, Rahman Md M, Bondad SE, Md B-D (2019) Impacts of salinity intrusion in community health: a review of experiences on drinking water sodium from coastal areas of Bangladesh. Healthcare 7:50. https://doi.org/10.3390/healthcare7010050
Sidike A, Zhao S, Wen Y (2014) Estimating soil salinity in Pingluo county of China using Quickbird data and soil reflectance spectra. Int. J. Appl. Earth Obs. Geoinf. 26:156–175
Skaggs T, Anderson R, Corwin D, Suarez D (2014) Analytical steady-state solutions for water-limited cropping systems using saline irrigation water. Water Resources Research 12:9656–9674
Slavich PG, Petterson GH (1993) Estimating the electrical conductivity of saturated paste extracts from 1:5 soil:water suspensions and texture. Aus J Soil Res 31:73–81
Slinger D, Tension K (2005) Salinity Glove Box Guide for NSW Murray and Murrumbidgee compiled. Industries, NSW Department of Primary
Sommerfeldt TG, Thompson MD, Prout NA (1984) Delineation and mapping of soil salinity in Southern Alberta from Landsat data. Can. J. Remote Sens. 10(2):104–110
Sonmez S, Buyuktas D, Okturen F, Citak S (2008) Assessment of different soil to water ratios (1:1,1:2.5,1:5) in soil salinity studies. Geoderma 144:361–369
Suarez DL (1989) Impact of agricultural practices on groundwater salinity. Agriculture, Ecosystems and Environment 26:215–227
Sumfleth K, Duttmann R (2008) Prediction of soil property distribution in paddy soil landscapes using terrain data and satellite information as indicators. Ecol. Indic 8(5):485–501
Sumner ME, Naidu R (1998) Sodic soils: Distribution, properties, management, and environmental consequences. Oxford University Press, New York
Taghadosi MM, Hasanlou M, Eftekhari K (2018) Soil salinity mapping using dual-polarized SAR Sentinel-1 imagery. International Journal of Remote Sensing 40:237–252. https://doi.org/10.1080/01431161.2018.1512767
Tao JM, Fan XW, Weng YL (2012) Soil salt content retrieval from ALI multi-spectral image based on GRNN (in Chinese). Mod. Surv. Mapp 35:10–12
The World Bank Group (2018) Climate risk country profile-Vietnam. https://climateknowledgeportal.worldbank.org/sites/default/files/2019-01/15077-VietnamCountryProfile.pdf.
U. S. Salinity Laboratory Staff (1954) USDA Handbook no. 60. Diagnosis and improvement of saline and alkali soils. Washington, D. C.: U. S. Government Printing Office.
Verma KS, Saxena RK, Barthwal AK, Deshmukh SN (1994) Remote sensing technique for mapping salt affected soils. Int. J. Remote Sens 15(9):1901–1914
Wang Y, Wang Z.X, Lian X.J, Xiao H, Wang L.Y, He H.D (2011) Measurement of soil electrical conductivity and relationship between soluble salt content and electrical conductivity in Tianjin coastal area. Tianjin Agricult Sci 17: 18–21.
Weng YL, Gong P, Zhu ZL (2010) A spectral index for estimating soil salinity in the Yellow River delta region of China using EO-1 Hyperion data. Pedosphere 20:378–388
Wiegand L, Rhoades JD, Escobar DE, Everitt JH (1994) Photographic and videographic observations for determining and mapping the response of cotton to soil salinity. Remote Sens. Environ. 49(3):212–223
Yang L, Huang C, Liu G, Liu J, Zhu A (2015) Mapping soil salinity using a similarity based prediction approach: a case study in Huanghe River Delta, China. Chinese Geographical Science, 1–12.
Zanter K (2016) Landsat 8 (L8) Data Users Handbook, LSDS-1574, Version 2.0, March 29.
Zhang T, Qi J, Gao Y, Ouyang Z, Zeng S, Zhao B (2015) Detecting soil salinity with MODIS time series VI data. Ecological Indicators 52:480–489
Zhang TT, Zeng SL, Gao Y, Ouyang ZT, Li B, Fang CM, Zhao B (2011) Using hyperspectral vegetation indices as a proxy to monitor soil salinity. Ecological Indicators 11:1552–1562

Publisher's Note